Wire Grid Metamaterial for Directive Emission

Joaquim J. Barroso[1], Antônio Tomaz[2], and Ugur C. Hasar[3]

[1] National Institute for Space Research (INPE), São José dos Campos, SP, Brasil
[2] Technological Institute of Aeronautics (ITA), São José dos Campos, SP, Brasil
[3] University of Gaziantep, Gaziantep 27310, Turkey

Abstract — **In this work are reported the electromagnetic properties of an arrangement of periodic metallic grids devised to provide in the 12.5-20.0 GHz frequency range a refractive index less than unity with view to enhance the functionalities of a Ku-band horn antennas. The ultra-refractive behavior of the metamaterial structure is demonstrated by the impedance and refractive index values retrieved from simulated scattering parameters.**

Key words: artificial dielectric; near-zero refractive index; metamaterial; antenna directivity enhancement.

Fig. 1. Refraction on the interface of a near-zero refractive index medium.

I. INTRODUCTION

Many works [1]-[6] have shown that metamaterials with near-zero refractive index are able to manipulate the flow of electromagnetic waves so as to produce a directive beam from antennas and radiating apertures, thus having a great potential for use in advanced communications systems. In typical designs these materials consist of periodic arrays of metallic structures that interact with electromagnetic waves in the same way as a homogeneous medium provided the lattice constant is smaller than a quarter of the operating wavelength. Such a limit is usually referred to as effective-homogeneity condition whereby refraction dominates over diffraction and scattering phenomena. When this condition is satisfied, the structure is electromagnetically uniform along the direction of wave propagation and thus can be characterized by well-defined constitutive parameters which are independent of the size of the material and, as will be shown, solely depend on nature of the unit cell.

The directivity enhancement of rays emitted from a source immersed in a medium with a refractive index, n, near zero is illustrated in Fig. 1. Because $n \approx 0$, all the rays emitted from the source would refract, by Snell's law, almost perpendicular to the material surface. With this motivation, the present work reports on the design of a metamaterial to provide a refractive index less than unity and with an average value of 0.5 in 12.5-20.0 GHz frequency range to enhance and control the directivity of microwave antennas.
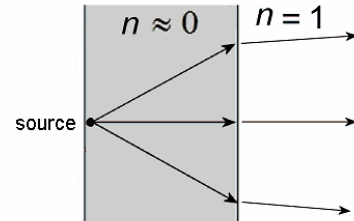
II. WIRE GRID STRUCTURE

Similar to the structure described in [2,4], the wire grid metamaterial investigated here is composed of three copper grids built up of 2x4 unit square cells, where each cell is repeated periodically in the x and y directions as illustrated in Fig. 2. Along the z direction, adjacent grids are separated by the periodic distance p; the grid spacing is implemented by embedding the metallic structure into a low-loss, rigid polystyrene foam, with dielectric constant of 1.03 and loss tangent $1.0\text{x}10^{-4}$ [7].

In the simplest Drude model, the strips of the metallic grid can be viewed as a gas of free electrons with no interband transitions and infinite relaxation time (no decay), such that an effective permittivity (relative) is expressed by [1]-[5]

$$\varepsilon = \varepsilon_h \left(1 - \frac{\omega_p^2}{\varepsilon_h \omega^2} \right) \qquad (1)$$

where ε_h is the permittivity of the host medium, and ω the frequency of the incident radiation; ω_p is the plasmonic angular frequency of the metal, and which depends essentially on the geometry of the unit cell. When $\omega_p < \omega$, n is a complex quantity thus leading to attenuation of the propagating wave; if $\omega_p > \omega$, n is real and the wave propagates through the medium without attenuation. For a non-magnetic medium, the effective refractive is given by $n = \sqrt{\varepsilon}$.
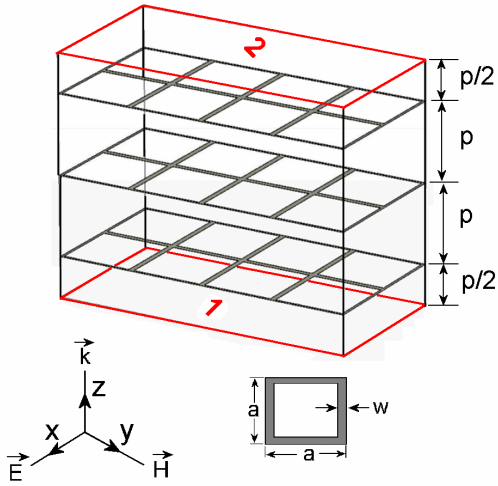
Fig. 2. Three-grid metamaterial (periodic distance p =5.8 mm), and geometric details of the unit square cell: side a = 5.9 mm, width w= 0.4 mm, and thickness 0.02 mm of the metallic strip. A plane wave with electric field polarized in the x-direction normally impinges onto port 1; ports 1 and 2 (reference and measurement planes) are placed half the periodic distance from the input and output grids.

III. ELECTROMAGNETIC SIMULATION

Full-wave electromagnetic numerical simulations using the CST MWS software [8] have been done to investigate the electromagnetic properties of the gridded structure devised in Fig. 2. Wave propagation takes place from ports 1 to 2, both parallel to the grids and perpendicular to the z-direction. For the boundary conditions, the front and back walls (parallel to the y-z plane) are set as perfect electric conductors, and the side walls (perpendicular to the x-y plane) as magnetic surfaces. For a pair of grids, magnitude and phase of the complex scattering parameters S_{11} and S_{21} are shown in Fig. 3, where it is noticed a sharp resonance dip at f_1= 17.40 GHz. Behavior of the phase of S_{11} gives further insight into the resonance process [Fig. 3(b)]. At the resonance the phase changes by π radians, from $-\pi/2$ to $+\pi/2$, as in a resonant RLC electric circuit. In the system with three grids, two frequencies of resonant transmission are identified (f_2=14.94 GHz, f_3=20.25 GHz) in Fig. 4. As expected, the appearance of two resonance frequencies is due to the fact that a periodic system with N sections forms N-1 coupled resonators. It is worth noticing that f_1 lies midway between f_2 and f_3.
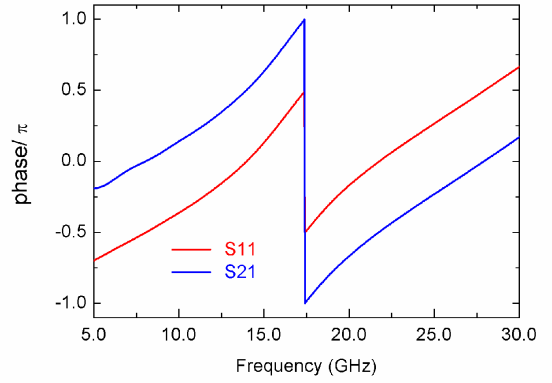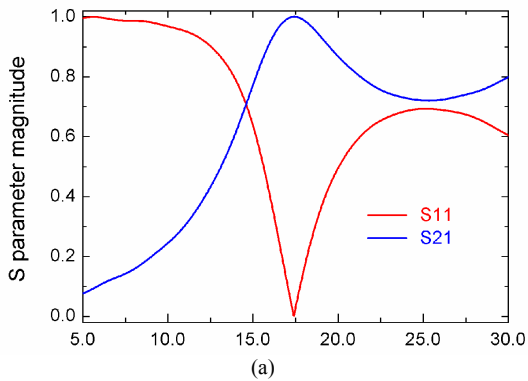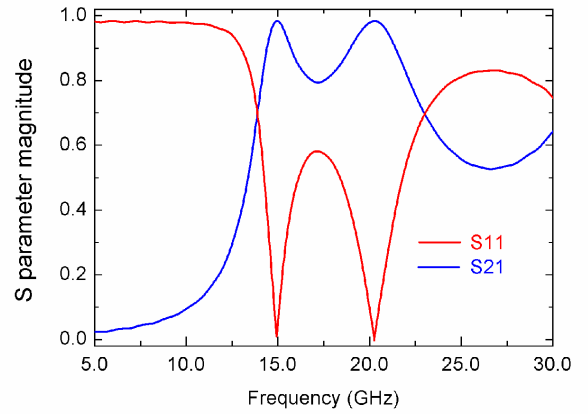

(a)

(a)

(b)

Fig. 3. (a) Magnitude and (b) phase of the S_{11} and S_{12} parameters simulated for the two-grid medium.
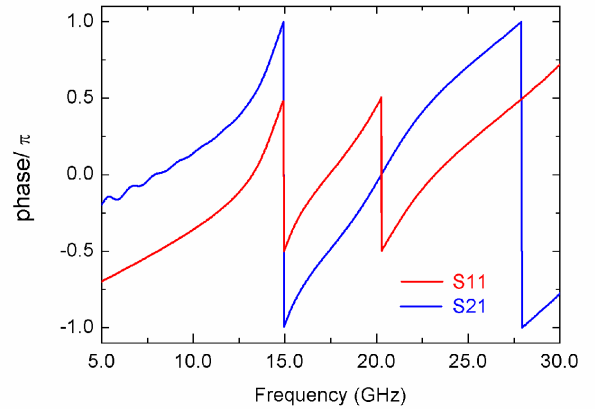

(b)

Fig. 4. (a) Magnitude and (b) phase of the S_{11} and S_{12} parameters simulated for the three-grid medium.

Since the grids are equally spaced, the fields of the lower frequency mode oscillate in phase in both resonators, while the fields of the higher frequency mode oscillate out of phase by π radians, as illustrated in Fig. 5. At this point and by visual inspection, we anticipate that the guided wavelength of the 2π-mode just corresponds to 2L, where L=3p is the length

of the slab; for the π-mode the guided wavelength is L. This issue will be examined quantitatively in Sec. V.
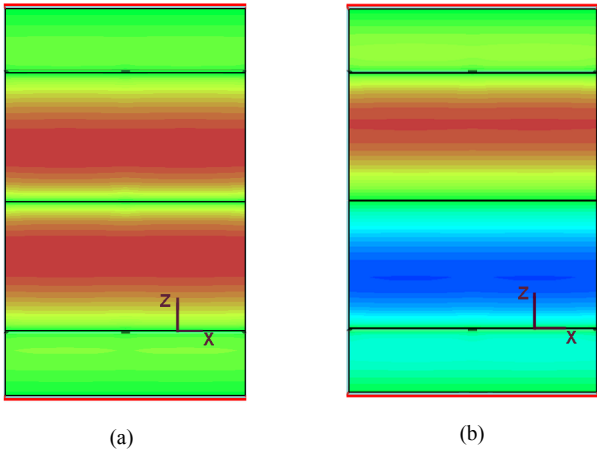

(a)   (b)

Fig. 5. Electric-field intensity patterns of the two resonant modes viewed on the x-z plane for the three-grid system. Distribution in (a) corresponds to the 14.94-GHz mode, for which Ez oscillates in the phase in the coupled resonators, often referred to as the 2π mode in slow-wave structures. Corresponding to higher frequency 20.25-GHz mode, in (b) the electric field Ez oscillates out of phase in the adjacent resonators, and commonly designated as π mode in accelerator structures. The intensity of the scale varies from 4 kv/m (red) to -4 kV/m (blue), with zero intensity being represented by green.

IV. RETRIEVAL OF IMPEDANCE, REFRACTIVE INDEX, AND CONSTITUTIVE PARAMETERS FROM SCATTERING PARAMETERS

The configuration in Fig. 2 constitutes a typical problem of determining the electromagnetic properties of a material from the forward and backward scattering parameters. Since the structure is reciprocal, because it is composed of passive elements, and assuming the time-harmonic variation exp(-iωt), implying that real parts of the wave impedance, z, and the refractive index of the medium, n, are both positive as required from the passivity condition, the complex S-parameters are written as [9]-[12]

$$S_{11} = S_{22} = \frac{\Gamma\left(1 - T^2\right)}{1 - \Gamma^2 T^2}, \quad S_{21} = S_{12} = \frac{T\left(1 - \Gamma^2\right)}{1 - \Gamma^2 T^2}, \quad (3)$$

where Γ is the intrinsic reflection coefficient at the free space-slab interface, and the T the transmission coefficient through the slab. These coefficients are expressed by

$$\Gamma = \frac{z - 1}{z + 1}, \quad T = e^{ik_0 nL}, \quad k_0 = 2\pi f/c \quad (4)$$

where k_0 is free-space wavenumber, L the length of the slab, f the operating frequency, and c the speed of light in vacuum. From (3) and (4) the electromagnetic parameters z are retrieved from the S-parameters as

$$z = \mp \sqrt{\frac{\left(1 + S_{11}\right)^2 - S_{21}^2}{\left(1 - S_{11}\right)^2 - S_{21}^2}}, \quad T = \frac{S_{21}}{1 - S_{11}\left(\frac{z - 1}{z + 1}\right)}, \quad (5)$$

$$n = \frac{1}{k_0 L}\left[\pm \left(\ln T\right)'' \pm 2\pi m - i\left(\ln T\right)'\right], \quad m = 0,1,2,3... \quad (6)$$

In (6), m is an integer denoting the branch indexes of the logarithm function, with $\ln(T)'$ and $\ln(T)''$ representing the real and imaginary parts of $\ln(T)$, respectively. Obtained from the S-parameters, the complex quantities {z, n} characterize the electromagnetic properties of a material and are used when discussing wave propagation. But in some cases, when discussing microscopic origin of electromagnetic effects, it is more convenient to use a second pair of analytic variables that impart a material interpretation, through the electrical and magnetic responses of the medium. Such quantities are the electric permittivity $\varepsilon = \varepsilon' + i\varepsilon''$ and magnetic permeability $\mu = \mu' + i\mu''$ and relate with {z, n} through

$$\varepsilon = n/z, \quad \mu = nz \quad (7)$$

satisfying the passivity requirements of $\varepsilon'' > 0$ and $\mu'' > 0$.

V. RESULTS AND DISCUSSION

The retrieved wave impedance (real part, z') in shown in Fig. 6, where two features are to be noted. The first is that the transmission band, determined by $z' > 0$, is delimited by lower and upper bounds at 12.5 GHz and 25.0 GHz. The second noticeable feature is the presence of two sharp dips at the resonance frequencies, with the dips approaching the impedance-matched value $z' = 1$. But such a strong variation at f_1 and f_2 does not manifest itself on the retrieved curve for the refractive index, which runs smoothly from the point P to B, as shown in Fig. 7. Point P, at 12.5 GHz, corresponds to the plasma frequency which explicitly appears in the Drude model, equation (1). Point B, at 25.0 GHz, indicates the Bragg frequency: a special frequency at which half the wavelength is equal the periodic distance, thus implying that the guided wavelength is just the free-space wavelength. In fact, since $k = n k_0$ we see that B is nearly close to $n = 1.0$. Also we note that a free-space wavelength of p=0.58 cm gives ~25.0 GHz. Above this frequency, diffraction effects dominate and the retrieved parameters produce unphysical artifacts as evidenced by the negative slope, which is common is metamaterial retrieval procedures. But in the low-frequency region, the retrieved curve is nicely fitted by the Drude curve up to f_2=14.94 GHz, n_2=0.58. This gives the guided wavelength λ_2=3.46 cm for which λ_2/L=2.0, where L=3p is the length of the three-grid slab. Also notice that $\lambda_2/4 > $ p, a condition that ensures effective-homogeneity. For f_3=20.26 GHz and n_3=0.85 we obtain λ_3=1.73 cm   and λ_3/L=1.0. In addition, we see that

the retrieved *n*-curves for 2- and 3-drid slabs are perfectly matched over the P-B frequency range, meaning that the retrieved refractive index, verified to be independent of length, may be interpreted as a local effective parameter. This conclusion equally holds for the wave impedance as displayed in Fig. 6.
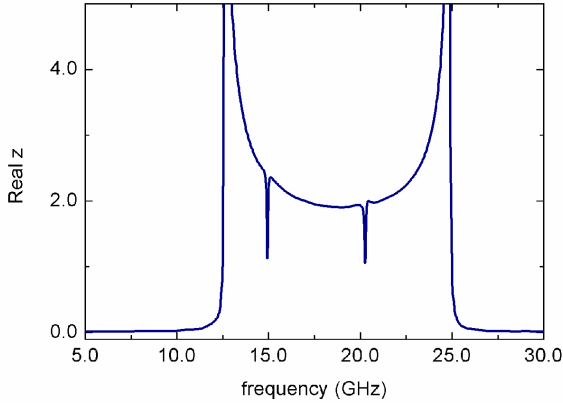

Fig. 6. Retrieved real part of the wave impedance for the slab with three grids; the two resonant dips are at f_2 =14.94 GHz and f_3 =20.26 GHz. For the slab with two grids, the corresponding curve coincides with the above curve but with a single dip at 17.40 GHz. Notice that the resonant dips approach the impedance-matched value $z' = 1$.
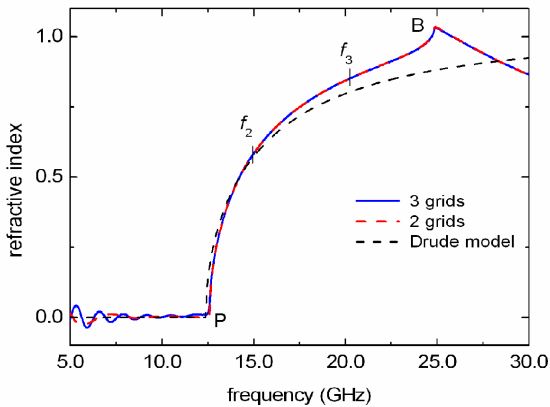

Fig. 7. Retrieved real part of the refractive index and the analytical curve from the Drude model. The points P and B indicate the plasma and Bragg frequencies, respectively.

The retrieved permittivity curve (Fig. 8) also shows a good agreement with the analytical one, especially in the plasma frequency branch (to the left of P) where ε' is negative. Two spikes appear at f_2 and f_3, with the ε' curve continuously diverging from the Drude curve. Apart from the spikes, such a divergence correlates well with the steadily increasing retrieved permeability (Fig. 9). Departing from a nearly-constant value in the low-frequency region, the μ' curve goes upwards until reaching the Bragg frequency, and then drops to negative values.
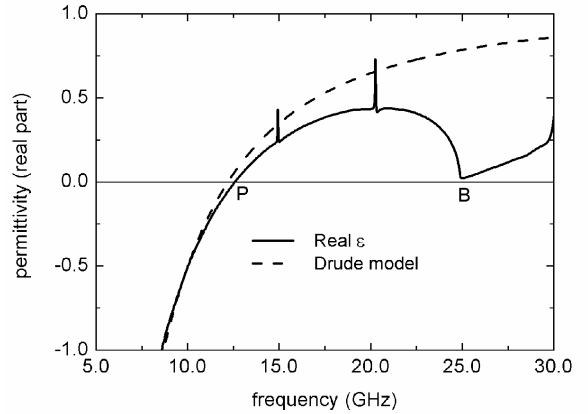

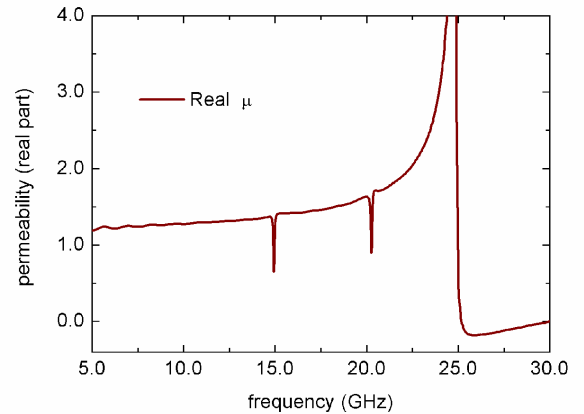Fig. 8 Retrieved real part of the permittivity and the Drude model curve.

Fig. 9 Retrieved real part of the magnetic permeability (relative to vacuum).

VI. APPLICATION IN ANTENNAS

To demonstrate the applicability of an epsilon-near-zero (ENZ) material, we present simulation results that show the improvement of the radiation characteristics of a horn antenna loaded with an ENZ material with a permittivity $\varepsilon \approx 0.01$. Figs. 10(a) and 10(b) compare an empty antenna with the same antenna with its aperture covered by an ENZ plate. It is clearly apparent in Fig. 10(a) that the intensity of the electric field radiated from the loaded antenna is far more directive. This effect is quantitatively shown in Fig.11, where on the E-plane radiation pattern, the side lobes of the loaded antenna appear to be significantly reduced
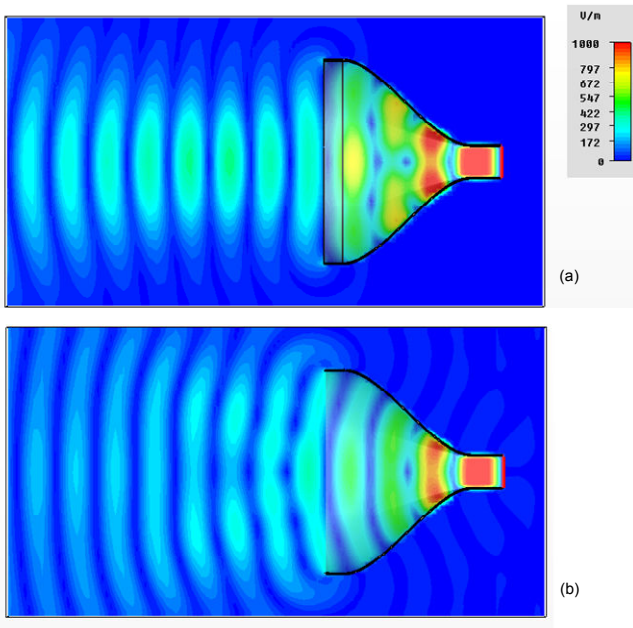
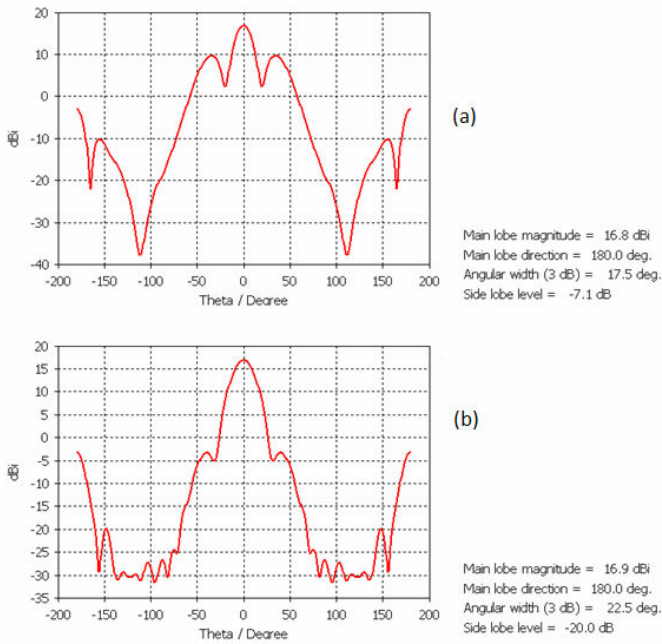Fig. 10. Distribution of the electric field radiated by (a) an ENZ loaded antenna and (b) an empty one.

Fig. 11. Radiation patterns (E-plane) for (a) the empty and (b) loaded antenna.

VII. CONCLUSIONS

Due to the resonant distances between the coupled grids, the spikes on the retrieved curves indicate the manifestation of interesting effects for which electric and magnetic responses are particularly strong at resonance. The increasing of the permeability with frequency likewise indicates magnetic activity developed in the gridded metamaterial. Although the Drude model assumes a non magnetic medium (μ =1), the excellent agreement between the analytical and retrieved curves ensures that the retrieved constitutive parameters have a proper physical meaning in the 12.5-20.0 GHz range and can be described as a homogeneous material with local effective parameters. In this sense, the engineered medium studied here can indeed be considered as an artificial dielectric with an average refractive index of 0.5 in the usable frequency range, thus enabling its application in Ku-band antennas.

REFERENCES

[1] G. V. Eleftheriades and N. Enghetta, "Metamaterials: fundamentals and applications in the microwave and optical regimes', *Proc. IEEE*, vol. 99, no. 10, pp.1618-1621, Oct. 2011.

[2] S. Enoch, G. Tayeb, P. Sabouroux, N. Guérin, P. Vicent, "A metamaterial for directive emission", *Phys. Rev. Lett.*, vol. 89, no. 21, Art. ID 213902, 2002.

[3] S. J. Franson and R. W. Ziolkowski, "Confirmation of zero-n behavior in a high gain grid structure at millimeter-wave frequencies", *IEEE Antennas Wireless. Propag. Lett.*, vol. 8, pp. 387-390, 2009.

[4] Q. Wu, P. Pan, F.-Y. Meng, L.-W. Li, J.Wu, "A novel flat lens horn antenna designed based on zero refraction principle of metamaterials", *Appl. Phys. A*, vol. 87, pp. 151-156, 2007.

[5] D. Bonefačić, S. Hrabar, D. Kvakan, "Experimental investigation of radiation properties of an antenna embedded in low permittivity thin-wire-based metamaterial", *Microw. Opt. Technol. Lett.*, vol. 48, no. 12, pp 2581–2586, Dec. 2006.

[6] Fan Yang and Y. Rahmat-Samii, "Reflection phase characterization of the EBG ground plane for low profile wire antenna applications", *IEEE Trans. Antennas Propag.*, vol. 51, no. 10, pp. 2691-2703, Oct. 2003.

[7] W. P. Wetsphal and A. Sils, " Dielectric constant and loss data", MIT Air Force Materials Lab, AFML-TR-72-36, 1972.

[8] CST Microwave Studio, Version 2005, CST GmbH, Darmstadt, Germany.

[9] J. J. Barroso and A. L. de Paula, "Retrieval of permittivity and permeability of homogeneous materials from scattering parameters", *J. of Electromagn. Waves and Appl.* , vol. 24, pp. 1563-1574, 2010.

[10] U. C. Hasar and J. J. Barroso, "Retrieval approach for determination of forward and backward wave impedances of bianisotropic metamaterials," *Prog. Electromagn. Res.*, vol. 112, pp. 109-124, 2011.

[11] J. J. Barroso and U. C. Hasar, "Constitutive parameters of a metamaterial slab retrieved by the phase unwrapping method," *J. Infrared Milli. Terahertz Waves*, vol. 33, no. 2, pp. 237-244, 2012.

[12] C. R. Simovski and S. A. Tretyakov, "Local constitutive parameters of metamaterials from an effective-medium perspective", *Phys. Rev. B*, vol. 75, Art. ID 195111, 2007.